nature neuroscience

Synaptic background activity controls spike transfer from thalamus to cortex

Jakob Wolfart[1,3,4], Damien Debay[1,4], Gwendal Le Masson[2], Alain Destexhe[1] & Thierry Bal[1]

Characterizing the responsiveness of thalamic neurons is crucial to understanding the flow of sensory information. Typically, thalamocortical neurons possess two distinct firing modes. At depolarized membrane potentials, thalamic cells fire single action potentials and faithfully relay synaptic inputs to the cortex. At hyperpolarized potentials, the activation of T-type calcium channels promotes burst firing, and the transfer is less accurate. Our results suggest that this duality no longer holds if synaptic background activity is taken into account. By injecting stochastic conductances into guinea-pig thalamocortical neurons in slices, we show that the transfer function of these neurons is strongly influenced by conductance noise. The combination of synaptic noise with intrinsic properties gives a global responsiveness that is more linear, mixing single-spike and burst responses at all membrane potentials. Because in thalamic neurons, background synaptic input originates mainly from cortex, these results support a determinant role of corticothalamic feedback during sensory information processing.

Thalamocortical neurons in the dorsolateral geniculate nucleus relay visual input from retinal ganglion cells to the cortex, from which they receive massive feedback[1,2]. The function and mechanisms of corticothalamic feedback are still a matter of discussion, but it is generally agreed that it has a strong influence on the transfer of sensory information by thalamocortical cells[3–7]. According to the classical view, thalamocortical cells function in two intrinsically generated firing modes. At depolarized membrane potentials, these neurons fire single action potentials, faithfully transmitting synaptic inputs. This relay or 'single-spike' mode is mainly found during the awake state[6,8]. At hyperpolarized potentials, activation of low-threshold calcium (T-type) channels triggers high-frequency bursts of action potentials[9,10]. The burst mode is mostly found during slow wave sleep and epileptic absence seizures, when thalamocortical cells participate in the synchronous bursting of the thalamic network, functionally uncoupling the cortex from visual input[8,11].

In vivo, neurons generally experience a noisy high-conductance state that is likely to interact with their built-in integrative properties[12,13]. Recent studies have shown that *in vivo*-like synaptic noise changes specific aspects of signal integration in cortical neurons[14–18]. Thalamocortical cells recorded *in vivo* are also in a high-conductance state, in particular during corticothalamic barrages[12,19]. A given thalamocortical cell receives between 4,000 and 8,000 synapses[20,21], of which ~30% have direct cortical origin[1,2,21,22]. In addition, they are innervated by intrathalamic inhibitory neurons (interneurons and reticular thalamic neurons), which also receive direct cortical inputs and account for ~30% of synapses onto thalamocortical cells[1,2,21–23]. Thus, ~60% of synapses of thalamocortical neurons are directly or indirectly related to the activity of corticothalamic axons (in addition to that of other afferents), but it remains uncertain whether, overall, this feedback is excitatory or inhibitory for thalamocortical cells[4]. It has been proposed that corticothalamic feedback could switch thalamocortical neurons between burst and single-spike modes[7,22,24,25], but it is also unclear whether corticothalamic input increases or decreases thalamocortical cell bursting[7]. We hypothesize that corticothalamic feedback exerts its function not (only) by exciting or inhibiting thalamocortical cells, but by using a separate 'channel' of modulatory information[16]: the variance of background synaptic input. To explore how synaptic noise affects thalamic neurons, we recorded from thalamocortical cells in brain slices using dynamic-clamp injection of stochastic background conductances. We found that background conductance noise significantly changed the 'burstiness' (percentage of burst responses per spike-evoking input) and the input-output transfer function of thalamic relay neurons.

RESULTS

Conductance noise and input simulation

We recorded from thalamocortical neurons in dorsolateral geniculate nucleus (LGNd) slices of guinea pigs, using intracellular electrodes and the dynamic-clamp technique[26]. We analyzed 52 neurons from 36 animals. These neurons had a resting potential ± s.e.m. of –63 ± 0.4 mV and an input resistance of 61 ± 4 MOhm and showed rebound burst discharges accompanied by low-threshold calcium spikes (LTS) upon repolarization after hyperpolarization (**Fig. 1a**, inset in 'Quiescent' graph). These properties[8,9,23], as well as morphological reconstructions

[1]Unité de Neurosciences Integratives et Computationnelles, Centre National de la Recherche Scientifique, 91198 Gif-sur-Yvette, France. [2]Institut National de la Santé et de la Recherche Médicale (INSERM) 358, Université Victor Segalen Bordeaux 2, Bordeaux, France. [3]Present address: Neurozentrum, Department of Neurosurgery, University Hospital Freiburg, Breisacher Strasse 64, 79106 Freiburg, Germany. [4]These authors contributed equally to this work. Correspondence should be addressed to T.B. (thierry.bal@iaf.cnrs-gif.fr) or J.W. (jakob.wolfart@unklinik-freiburg.de).

Received 14 July; accepted 30 September; published online 30 October 2005; doi:10.1038/nn1591

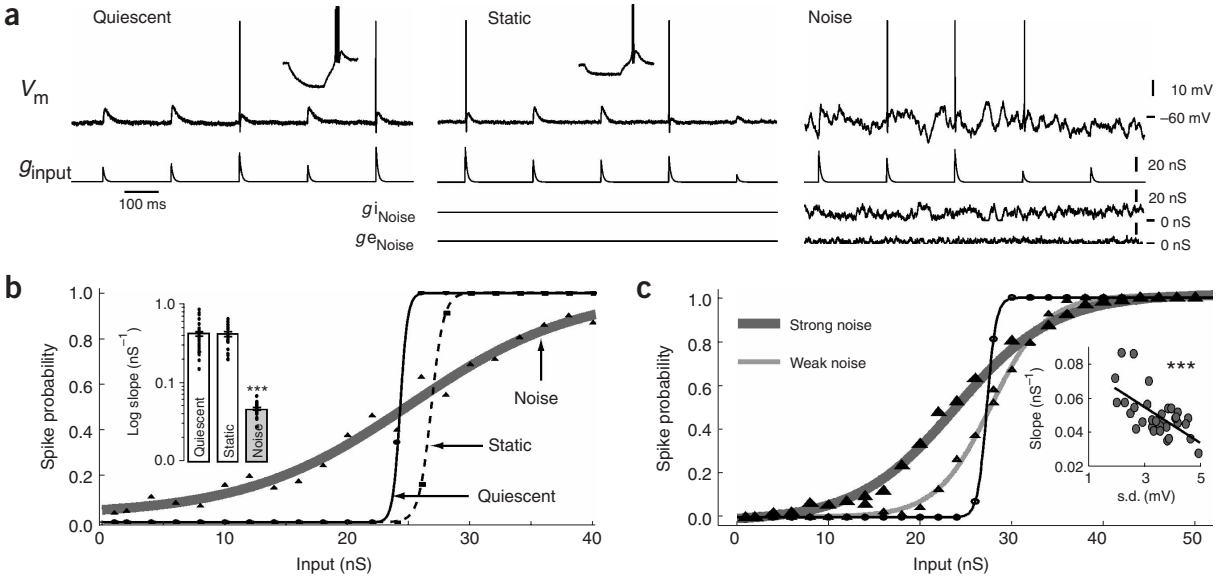

Figure 1 The influence of conductance (*g*) noise changes the transfer function of thalamocortical cells recorded *in vitro*. (**a**) Voltage during injection of input *g* alone (g_{input}, Quiescent) and with additional inhibitory plus excitatory background *g* strengths (gi_{Noise}, ge_{Noise}) that were either non-fluctuating (Static) or stochastically fluctuating (Noise). Combined noise *g* reduced the input resistance to ~50% (insets in Quiescent, Static). (**b**) Probabilities of input *g* strengths to evoke ≥1 spike, fitted to sigmoid functions. Noise, but not Static, induced a gain (slope) reduction of the response curve (inset). (**c**) Decreasing the variance of noise *g* values (Strong, Weak) increased the input-output slope. The response gain was correlated with the noise-induced voltage variance (s.d.). Error bars, s.e.m.

of biocytin-filled cells, unambiguously identify the neurons as thalamocortical relay neurons.

The standard protocol used to assess the integration properties of thalamocortical cells consisted of a recording at resting potential, where excitatory signal input conductances were injected at 5 Hz without additional background conductances (**Fig. 1a**, Quiescent). Subsequently, we added excitatory and inhibitory background conductances without fluctuations (**Fig. 1a**, 'Static'). The total background conductance was adjusted such that the cells' input resistance was approximately 50% of its initial value (**Fig. 1a**, compare insets of Quiescent and Static traces), similar to the 'shunting' effect observed in thalamocortical cells *in vivo* during the activation of corticothalamic projections[19]. We then injected the same background conductances with stochastic fluctuations (**Fig. 1a**, 'Noise'). To separate the effect of noise from simple depolarization or hyperpolarization, we compensated, when necessary, for the effect of background conductances by injecting a small DC current such that the mean potential was similar under these conditions (**Fig. 1a**). The variance of the membrane potential was low in the quiescent (0.71 ± 0.03 mV) and static conditions, and was increased with noise (3.65 ± 0.13 mV, $n = 24$) to an amplitude consistent with voltage fluctuations *in vivo*[19,27].

Noise affects the gain of thalamocortical neurons

We assessed whether inputs were transmitted and how this transfer was affected by synaptic background noise by evaluating the probability that a given input magnitude would evoke at least one action potential within a 20-ms delay[17] for the quiescent, static and noise conditions (**Fig. 1b**). The slope (gain) of the input-output relation was determined by fitting a sigmoid function to spike probability values and extracting its slope at the 0.5 probability. Although a step-like transfer function characterized the quiescent and static conditions, under the influence of noise the response probability was linearized, adopting intermediate values between 0 and 1 over a larger input range (**Fig. 1b**). The gain was not significantly different between the quiescent and static conductance injections, but was strongly reduced with noise (inset in **Fig. 1b**; quiescent: 0.413 ± 0.029 nS^{-1}, $n = 41$; noise: 0.046 ± 0.002 nS^{-1}, $n = 27$; static: 0.409 ± 0.029 nS^{-1}, $n = 24$; quiescent versus noise: $P < 0.001$; quiescent versus static: $P = 0.72$). We obtained similar results using a measure of the total spike output (see Methods). Thus, consistent with previous results from the cortex[14,16,17], the variance of background conductance reduced the input-output gain of thalamocortical cells and increased the cells' sensitivity to small inputs.

Because the effect of corticothalamic feedback is expected to vary considerably with the state of the animal and the signals that are processed[7,22,28], we explored different variances of the fluctuating conductances. In the 'strong noise' condition (our default for the results described above), the conductance variances for excitatory and inhibitory noise were 3 nS and 12 nS, respectively. A decrease in noise conductance variances (to 1 and 4 nS, respectively; 'weak noise' voltage variance: 2.61 ± 0.14 mV, $n = 5$) increased the input-output gain (**Fig. 1c**, 0.070 ± 0.007 nS^{-1}, $n = 5$; versus 'strong noise': 0.046 ± 0.002 nS^{-1}, $n = 27$; $P < 0.01$). The gain in the various noise conditions correlated with the actual degree of voltage variance induced by the noise (**Fig. 1c**, inset, $n = 33$, $r = 0.63$, $P < 0.01$). These results show that background synaptic activity is able to modulate the response curve of thalamocortical neurons in a multiplicative manner.

Gain depends on membrane potential and input frequency

The responsiveness of thalamic neurons at depolarized membrane potentials is entirely different from that at hyperpolarized potentials[8,9,29]. At hyperpolarization, incoming excitatory postsynaptic potentials (EPSPs) can be amplified by T-type channels producing LTS burst discharges[29]. We found that, unexpectedly and unlike what is observed for cortical cells[17], the gain of thalamocortical cells at hyperpolarized potentials was markedly lower than that at depolarized

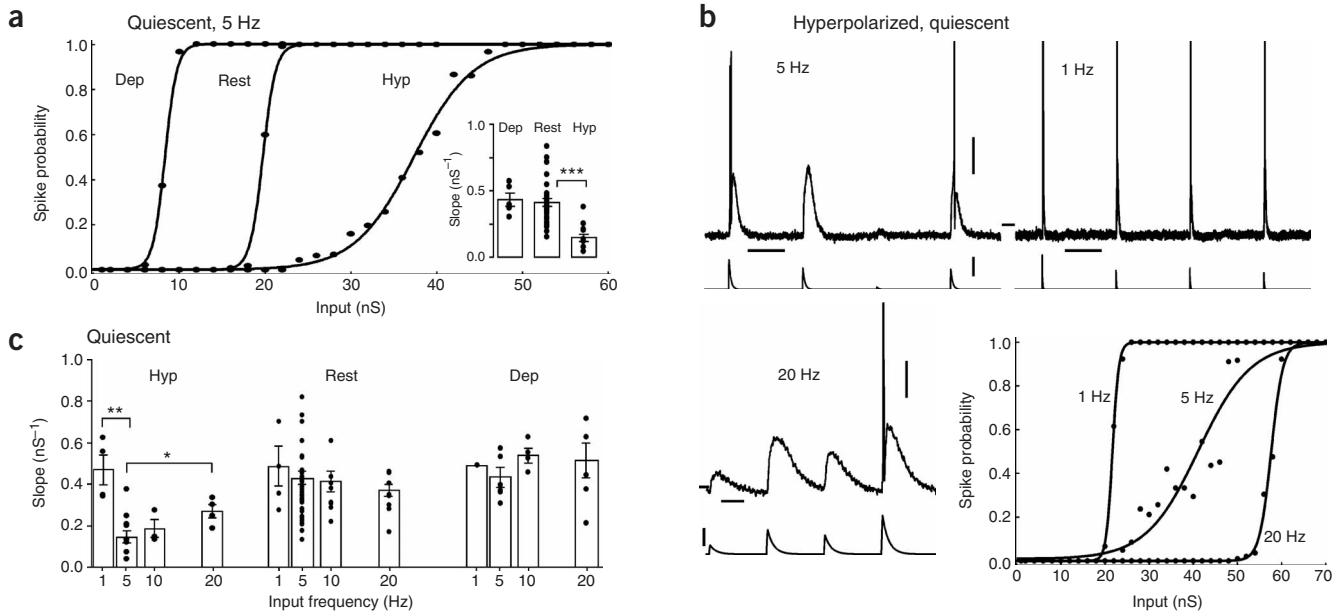

Figure 2 Voltage and frequency dependence of the response gain of thalamocortical cells, without noise. (**a**) Response curves during quiescent mode, 5 Hz stimulation, at depolarized (Dep), resting (Rest) and hyperpolarized potentials (Hyp). The response gain (slope) was equal at Dep and Rest but reduced at Hyp (inset). (**b**) Different input frequencies (5 Hz, 1 Hz, 20 Hz) in the Hyp, quiescent condition. Response curves showed lower gain only in the 5 Hz condition. Scale bars in **b**: horizontal below traces: 5 Hz, 0.1 s; 1 Hz, 0.5 s; 20 Hz, 20 ms; between traces: –70 mV; vertical (upper, lower): 10 mV, 20 nS. (**c**) Summary of experiments as in **a** and **b**. Response gains were all-or-none with all input frequencies at Rest and Dep and with 1 Hz at Hyp, but they were reduced at Hyp with 5 Hz and 10 Hz inputs. Error bars, s.e.m. * $P < 0.05$, ** $P < 0.01$, *** $P < 0.001$.

and resting potentials (**Fig. 2a**, hyperpolarized: 0.146 ± 0.028 nS^{-1}, $n = 12$; resting: 0.413 ± 0.029 nS^{-1}, $n = 41$; $P < 0.001$).

What could cause the voltage dependence of gain? T-type channel activation at hyperpolarization is not expected to reduce the gain but rather to increase the all-or-none character of thalamocortical cell responses[22]. Yet, because de-inactivation time constants of T-type channels are in the range of hundreds of milliseconds[9,30], varying degrees of T-type channel recruitment are to be expected at a 5-Hz input rate with randomized EPSP amplitudes. This could account for the gain reduction. Further analysis showed that much of the LTS variability at hyperpolarization could indeed be attributed to the recent LTS activation history (**Supplementary Fig. 1** online).

These results suggest that the voltage dependence of gain in the quiescent neuron is itself dependent on the input frequency. We tested four input frequencies (1, 5, 10 and 20 Hz) at all voltage conditions. At resting and depolarized potentials, there was no frequency dependence of gain (ANOVA, $P = 0.29$). However, at hyperpolarization, a frequency dependence of gain was clearly visible (**Fig. 2b,c**, ANOVA, $P < 0.001$). This is in agreement with the idea that the voltage and frequency dependence of gain were due to the T-type channel gating behavior: the low gain at hyperpolarization reverted to an all-or-none gain when the input frequency was lowered to 1 Hz such that T-type channels could recover from inactivation between stimuli[30] (**Fig. 2b,c**; 1 Hz: 0.468 ± 0.072 nS^{-1}, $n = 4$; 5 Hz: 0.146 ± 0.028 nS^{-1}, $n = 12$; 1 Hz versus 5 Hz: $P = 0.008$). On the other hand, increasing the input frequency to 10 Hz and 20 Hz gradually increased the gain at hyperpolarization (**Fig. 2b,c**; 20 Hz: 0.270 ± 0.033 nS^{-1}, $n = 4$; 20 Hz versus 5 Hz: $P = 0.039$). This effect could be explained by a cumulative inactivation of the T-type channels at higher frequencies: the inability of T-type channels to follow high frequencies endows thalamocortical cells with low-pass filter properties when they are hyperpolarized[29]. Thus, our results suggest the following scenario: at hyperpolarization and input frequencies around 5 Hz, T-type channels favor low gain transfer functions, whereas at more depolarized potentials, thalamocortical cells are expected to show all-or-none gain regardless of the input frequency.

Noise renders gain independent of voltage and frequency

To test how conductance noise may interfere with the voltage and frequency dependence of gain, we performed the characterization described earlier (**Fig. 2**) in the presence of noise (**Fig. 3**). The injection of noise reduced the gain at all voltage conditions (**Fig. 3a**). Unlike in the quiescent condition, the gain was very similar at all membrane potentials, although still slightly reduced at hyperpolarization with a 5 Hz input (inset in **Fig. 3a**; see also inset in **Fig. 3c**: ANOVA voltage dependence: $P = 0.007$; across all frequencies, $P = 0.076$; with frequencies pooled, $P = 0.145$). Thus, the voltage dependence of gain was strongly reduced with noise.

We next asked if the frequency dependence of gain that was found in the quiescent conditions would endure in the noise condition. In accordance with the hypothesis that voltage and frequency dependence resulted from the same mechanism, noise nearly abolished the frequency dependence of gain. We compared three input frequencies at hyperpolarized potentials in the presence of noise (**Fig. 3b**; compare with **Fig. 2b**). The marked distinction in gain between 1 Hz and 5 Hz and between 5 Hz and 20 Hz (**Fig. 2c**) was much reduced with noise (**Fig. 3c**, Hyp). At all other frequencies and membrane potentials, the gain was equally low when noise was present (**Fig. 3c**, ANOVA across all conditions; frequency dependence, $P = 0.049$; with potentials pooled, $P = 0.087$). Further analysis of the underlying events showed that noise increased the variability of subthreshold responses to an overall high level, overwhelming the variability due to LTS, thereby reducing the response gain of thalamocortical cells to an overall low level that was equal across different membrane potentials and input frequencies

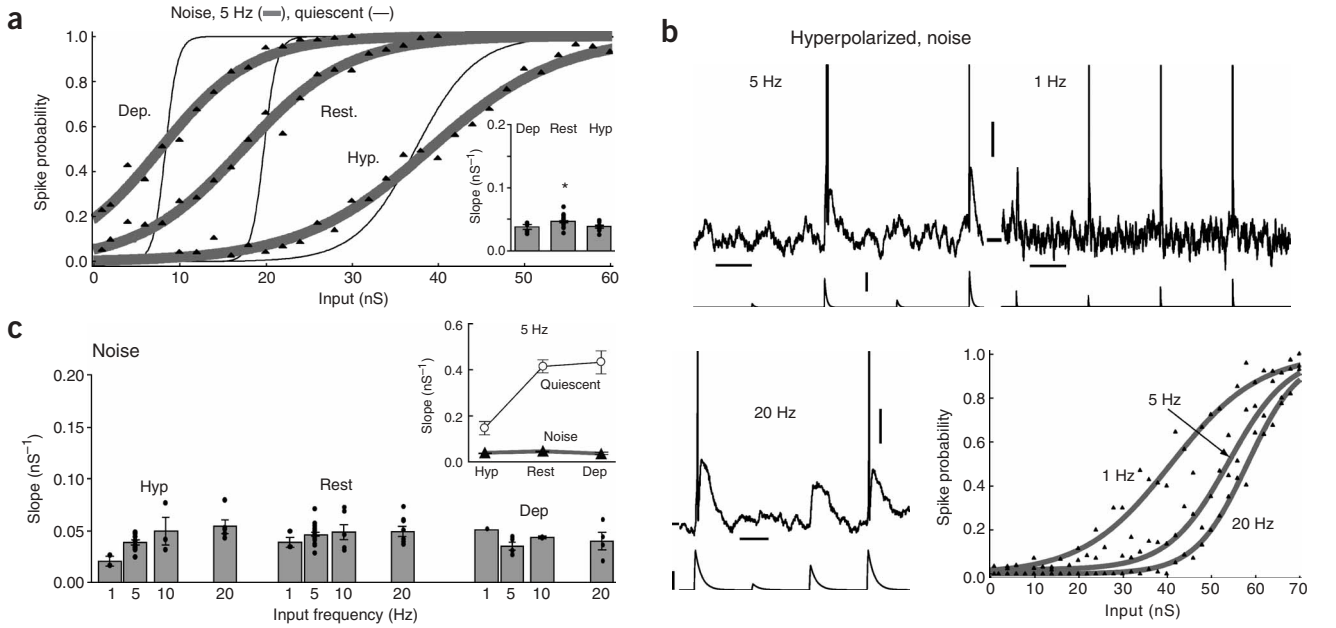

Figure 3 Influence of noise on voltage and frequency dependence of gain. (**a**) Thick gray curves: response probabilities during noise mode, 5 Hz stimulation, at depolarized (Dep), resting (Rest) and hyperpolarized potentials (Hyp). Thin black lines: quiescent curves from **Figure 2a** (same cell). The response gain (slope) during noise was almost equally low at all potentials (inset). (**b**) Different input frequencies (5 Hz, 1 Hz, 20 Hz) in the Hyp, noise condition. Response curves showed almost equally low gain at all input frequencies. (**c**) Summary of experiments as in **a** and **b**. Response gains were low at all input frequencies and membrane potentials. Compare to **Figure 2c** (note: *y*-axis scaling different). The inset shows loss of voltage dependence of gain in the noise compared to the quiescent condition (at 5 Hz input). Scale bars in **b**: horizontal below traces: 5 Hz, 0.1 s; 1 Hz, 0.5 s; 20 Hz, 20 ms; between traces: –70 mV; vertical (upper, lower): 10 mV, 20 nS. Error bars, s.e.m.

(**Supplementary Fig. 1**). Thus, noise effectively masked the intrinsic, nonlinear response behavior of thalamocortical cells and equipped them with a robust, voltage-independent transfer function.

Stimulation with physiologically realistic inputs

Mean firing frequencies of retinal ganglion cells *in vivo* are in the range of 5–50 Hz and are gamma or Poisson distributed[31]. Even if the magnitude of a single retinogeniculate EPSP may vary little, the 'effective' retinogeniculate EPSPs depend, among other factors, on variable degrees of temporal summation, such that the effective input has a larger magnitude range[32,33]. In the experiments described so far, the variability of the effective input was achieved by randomizing the input conductances while fixing the input frequency, thereby separating magnitude from frequency and thus allowing better control and comparison with cortical neurons[17]. To check whether the spike probability is voltage and frequency dependent under more physiological input conditions, we compared the response properties of thalamocortical cells during stimulation with Poisson-distributed 'retinal' input using a mean frequency of 10 Hz. Even though the retinogeniculate input conductance was fixed, Poisson-rate stimulation led to varying effective input EPSP magnitudes as a result of summation (**Fig. 4a**). At the beginning of each experiment, the conductance magnitude was adjusted such that evoked subthreshold EPSPs at resting potential were in a physiological range (5–15 mV)[32]. Because the degree of input summation is dependent on the frequency, we used the inter-stimulus interval (ISI) immediately preceding the response to measure input strength (**Fig. 4b**).

At resting potential, with subthreshold input magnitude, spikes were evoked only by summed inputs at smaller ISIs (**Fig. 4a**,**b**): ISIs in the range of 50–600 ms were related to spike probabilities in the range of 0 to 0.021 ± 0.016 ($n = 4$), whereas ISIs shorter than 50 ms were associated with a spike probability of 0.530 ± 0.123 ($n = 4$). In contrast, at hyperpolarization, spike response could be evoked not only by input summation, but also by long ISIs (**Fig. 4a**,**b**; ANOVA, $P < 0.001$): ISIs in the range of 300 ms to 600 ms were related to spike probabilities in the range of 0.253 ± 0.099 to 0.847 ± 0.061 ($n = 4$), even higher than those evoked by ISIs shorter than 50 ms (0.398 ± 0.089, $n = 4$). Thus, consistent with our experiments using fixed input frequencies and randomized input magnitudes, spike probabilities induced by Poisson rate input had an all-or-none character at resting potential but adopted intermediate values, depending on input frequency, at hyperpolarized potentials.

We repeated the Poisson rate experiment described above, in the presence of noise (**Fig. 4c**,**d**). With noise, input summation also increased the spike probability at resting and hyperpolarized potentials. However, unlike in the quiescent condition, larger ISIs did not lead to different spiking probabilities at the hyperpolarized potential as compared to the resting potential (ANOVA, $P = 0.43$). Although no direct comparison between fixed rate and Poisson rate experiments (such as comparing the gain) is feasible, these results match: in both experimental conditions, voltage and frequency dependencies were abolished with synaptic background noise.

Noise increases burst firing

Action potential–burst firing in thalamocortical cells is classically considered to be the result of LTS activation after hyperpolarization[34–36]. However, in the noise condition, even at resting and depolarized potentials, high-frequency burst responses often occurred (**Fig. 5a**, left). Because noisy voltage fluctuations hamper LTS identification, we used a burst detection algorithm[35] (see Methods) to assess burstiness. Indeed, not only the voltage but also the presence of noise influenced burstiness (ANOVA, $P < 0.001$). At resting and depolarized

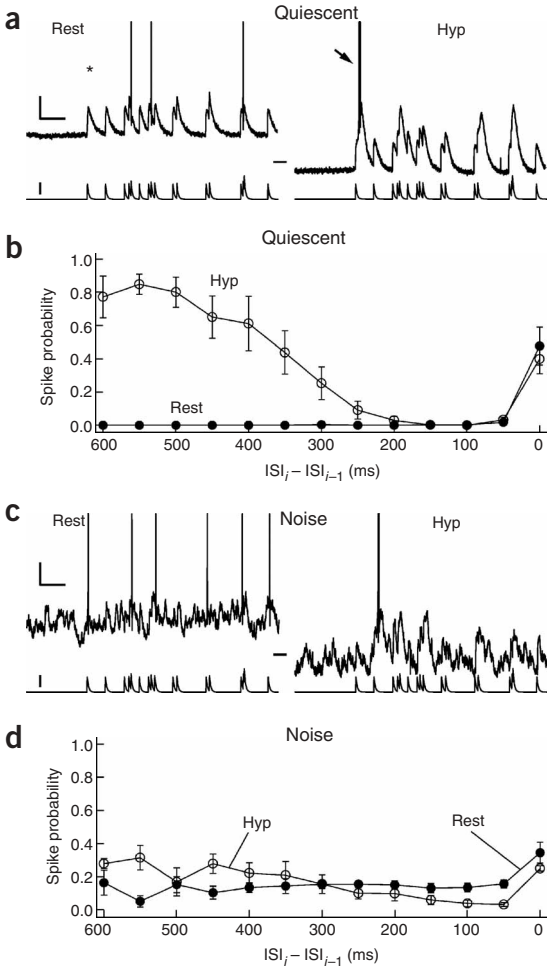

Figure 4 Physiologically realistic Poisson-distributed inputs. (**a**) Retinogeniculate input conductances (lower traces) were injected at a fixed magnitude with Poisson-distributed rate (mean frequency, 10 Hz). At resting potential (Rest) without synaptic noise, action potentials were only evoked by summation of inputs occurring at short interstimulus intervals (ISIs) whereas inputs with long ISIs did not trigger action potentials (left panel, asterisk). At hyperpolarized potential (Hyp), subthreshold inputs led to variable degrees of EPSP summation occasionally accompanied by LTS activation. Large ISIs led to the activation of LTS-driven bursts (right panel, arrow). (**b**) The probability of evoking at least one spike was plotted against the ISIs. Whereas at resting potential spiking probability was increased only with high-frequency inputs, at hyperpolarized potentials the spiking probability increased strongly with low frequency inputs. (**c**,**d**) During the injection of noise, the difference in frequency-dependent response behavior of thalamocortical cells was strongly reduced. Spiking probabilities were approximately equal at all input frequencies in the presence of noise. Scale bars in **a**,**c**, 100 ms, 10 mV; lower trace, 10 nS; between traces, –80 mV. Error bars, s.e.m.

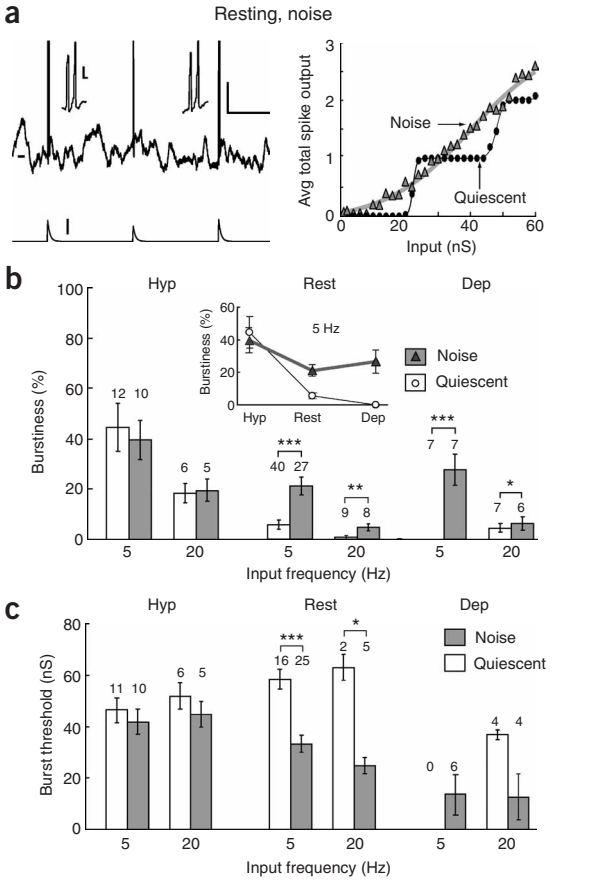

Figure 5 Noise increases occurrence of bursts at resting potential. (**a**) With noise, high-frequency bursts of action potentials occurred at resting potential (left). Plotting the average total number of spikes per burst response (**Supplementary Methods** online) against the input shows that noise linearized the staircase-like transfer function across the whole input range (right). (**b**) Percent bursts per spike-evoking stimulation with different input frequencies and membrane potentials. Noise increased burstiness at resting and depolarized potentials (for example, at 5 Hz, inset). This effect was smaller with higher input frequencies. Noise did not increase the burstiness at hyperpolarization. (**c**) The input value at which bursting occurred (burst threshold) was decreased with noise at rest and depolarization but not at hyperpolarization. Scale bars in **a**, 100 ms, 10 mV; lower trace, 10 nS; before trace, –80 mV; inset, 10 mV, 1 ms. Error bars, s.e.m. $^*P < 0.05$, $^{**}P < 0.01$, $^{***}P < 0.001$.

potentials, there was an increased burstiness with noise in 24 of 27 cases (**Fig. 5b**, inset; resting quiescent, 5 Hz: 5.7 ± 1.9%, $n = 40$; versus noise: 21.2 ± 3.4%, $n = 27$; $P < 0.001$; depolarized quiescent, 5 Hz: 0%, $n = 7$; versus noise: 27.6 ± 6.1%, $n = 7$; $P = 0.004$). As expected, burst firing was more pronounced at hyperpolarization (5 Hz quiescent: 44.5 ± 9.6%, $n = 12$), and there was no clear change of burstiness with noise (**Fig. 5c**, left). Another approach to quantifying burstiness is to determine the 'burst threshold': that is, the input level at which bursts first occur. This analysis again showed that at resting and depolarized potential, bursting was more likely with noise because the bursting threshold was much lower than in the quiescent condition (**Fig. 5c**, resting quiescent, 5 Hz: 58.5 ± 3.8 nS, $n = 16$; versus noise: 33.3 ± 3.4 nS, $n = 25$; $P < 0.001$; depolarized quiescent, 5 Hz: no bursting; versus noise: 13.5 ± 8.0 nS, $n = 6$).

What could be the reason for the increased burstiness with noise? In principle, a decrease in the membrane time constant resulting from conductance increase could have a role; however, no increased burstiness was detected in the static condition (burstiness at resting quiescent, 5 Hz: 6.2 ± 3.3%; versus at static: 6.5 ± 3.3%; $n = 22$; paired test: $P = 0.44$). The mean membrane potentials in the noise and quiescent conditions were not significantly different (resting quiescent, 5 Hz: –65.3 ± 0.8 mV; versus noise: –65.7 ± 0.8 mV; $n = 24$; paired test: $P = 0.80$), arguing against a role of T-type channels. Indeed, the gating parameters of T-type channels suggest little involvement in these

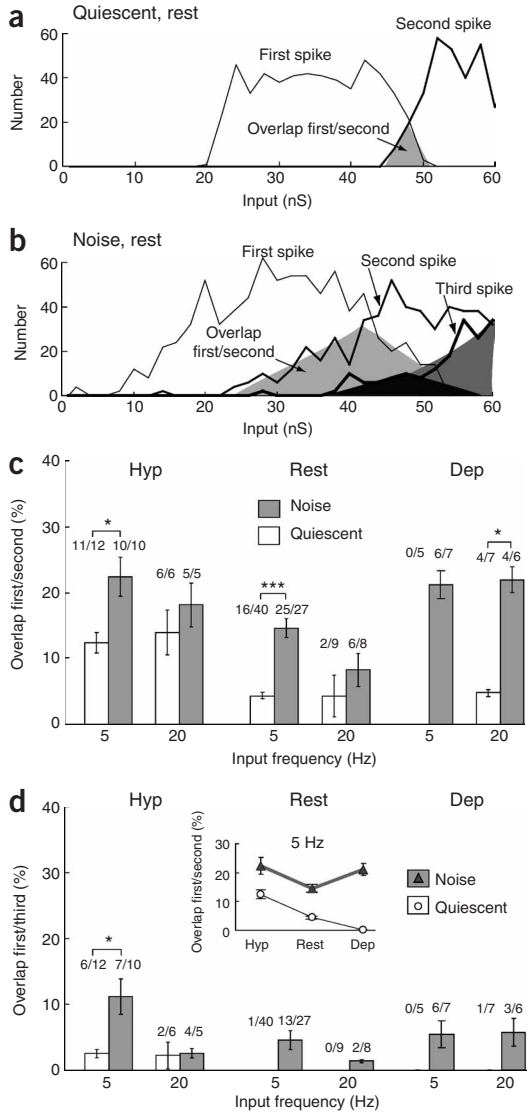

Figure 6 Noise mixes single-spike and burst responses of thalamocortical neurons. (**a**) Example of input strength distributions evoking single-spike (first spike) and burst responses (second spike, with interspike intervals $\leq$5 ms). Without noise, only very strong inputs could evoke spike doublets. (**b**) With noise, most input levels could evoke single-spike and burst responses. Different shades of grey mark areas of overlap between first and second spikes (light), second and third spikes (middle) and first and third spikes (dark). (**c**,**d**) Mixing (overlap) of single-spike and multiple-spike responses: (**c**) first and second spikes; (**d**) first and third spikes. Noise increased the mixing of single-spike and burst responses at most potentials and input frequencies (for example, at 5 Hz, inset). Error bars, s.e.m. $^{*}P < 0.05$, $^{***}P < 0.001$.

conditions[30], although native T-type currents of thalamic neurons can be available at resting potential[37]. We compared spike-triggered averages (STAs) of single-spike and burst responses during noise at the resting potential and observed that there was a small but significant difference in the pre-response voltage (**Supplementary Fig. 2** online). This suggests that even if, overall, noise has no effect on the membrane potential, short hyperpolarizations preceding inputs statistically recruit more T-type channels as compared to the situation in the quiescent state. In addition, the occasional occurrence of noise-induced depolarizations with retinal inputs clearly facilitated bursts, as seen from spike-triggered averages of excitatory and inhibitory conductances (**Supplementary Fig. 2**). These results show that noise increases the occurrence of burst responses at resting and depolarized potentials but not at hyperpolarized potentials.

Noise mixes single-spike and burst responses

If the number of spikes in the response grew proportionally with the strength of the input, the spike count could be used to reliably encode sensory information. Without synaptic background, such a reliable transfer function does not exist in the resting and depolarized states; the cell behaves as a high-pass filter, detecting only strong inputs with no discrimination of strength past a threshold (see the step-like response in **Fig. 5a**, right). Noise made cells generate, on average, a number of spikes proportional to input strength (**Fig. 5a**, right), providing a more linear transfer function at all potentials. Thus, in the presence of synaptic background activity, probabilistic 'mixing' of single-spike and burst responses potentially provides better encoding capabilities.

To quantify this mixing, we separated single-spike responses from responses with two- and three-spike bursts. We counted the different responses at the respective input levels and plotted their distribution (**Fig. 6a**,**b**). We calculated the relative overlap of the one-, two- and three-spike response curves by integration and compared the 'percent mixing' (overlap) for the different conditions (**Fig. 6c**,**d**). With noise, at resting potential, the overlap of one- and two-spike response curves was increased (**Fig. 6a–c**, 5 Hz quiescent: $4.3 \pm 0.52\%$, $n = 16$; versus noise: $14.6 \pm 1.4\%$, $n = 25$; $P < 0.001$). In the quiescent condition, only 16 of 40 cells showed two-spike bursts and one cell showed three-spike bursts with very strong inputs. In contrast, with noise, 25 of 27 cells showed two-spike bursts and 13 showed three-spike bursts; the overlap of the latter was zero in the quiescent condition but notable in the noise condition (**Fig. 6d**, $4.6 \pm 1.4\%$). The same difference in the mixing of single-spike and burst responses was true for depolarized and hyperpolarized potentials, although it was less marked for the latter (**Fig. 6c**,**d**; inset in **d**). At 20-Hz input, the difference in percent mixing was generally reduced (**Fig. 6c**,**d**). Thus, although thalamocortical cells recorded *in vitro* are usually either in single-spike mode or in burst mode[8], our data suggest that thalamocortical cells under the influence of synaptic background activity may show both burst firing and single-spike responses.

DISCUSSION

The main findings reported here are that (i) the duality of burst and single-spike modes in thalamic relay neurons is strongly affected by the presence of synaptic background activity and (ii) the input-output transfer function is determined by synaptic background activity combined with intrinsic properties. Previous work has shown that understanding the responsiveness of central neurons requires a detailed knowledge of their intrinsic properties, which are mediated by various calcium- and voltage-dependent conductances[10]. Our present results suggest that background activity alters this responsiveness fundamentally. We suggest that a complete characterization of the properties of central neurons requires the knowledge of intrinsic and synaptic background conductances, as well as the amount of conductance fluctuations (noise).

The dichotomy of burst and single-spike firing modes is based on recordings performed *in vitro* or *in vivo* during states of deep anesthesia (with slow waves in the electroencephalogram (EEG))[23]. During EEG-activated states, there is a sustained synaptic activity in thalamocortical cells[23,38], which accounts for about 50% of their input conductance[19]. We found here that if such states are recreated artificially using the

dynamic clamp, the distinction of firing modes is dramatically reduced: single-spike and burst firing seem to be mixed. Classically, burst firing in thalamic neurons has been invariably associated with hyperpolarization, and observations of bursts in awake, behaving animals[36,39] were difficult to reconcile with the fact that thalamocortical cells are depolarized in this state[39,40]. Our findings suggest that bursts should be observable if thalamocortical cells are depolarized, such as in awake animals, but only with sufficient levels of synaptic background activity.

Another consequence of synaptic noise is that it causes qualitative and quantitative changes in the responsiveness of thalamic neurons to external inputs. The response curves of thalamic neurons are very different in these simulated activated states compared to in the quiescent states. There is a multiplicative scaling by noise, leading to gain reduction and increased responsiveness to small inputs, similar to model predictions[14,27] and results from dynamic-clamp experiments in cortical neurons[16,17]. It may be explained by the fact that the probability for small-amplitude inputs to evoke a spike can only be enhanced by noise (floor effect), whereas for higher inputs, the probability can only be reduced by noise (ceiling effect)[17]. An important difference from the cortex is that in quiescent thalamocortical cells, the gain is highly dependent on membrane potential and input frequency; the low-threshold calcium current boosts the response specifically at hyperpolarized levels. With noise, this voltage-dependent response behavior is nearly eliminated, and the gain is similar at all potentials. Thus, the combination of intrinsic properties (T-type calcium current) and synaptic noise enables relay neurons to keep a uniform responsiveness for a large input range at different membrane potentials and, in this sense, to perform a particularly robust relay of information.

During sleep, thalamocortical cell bursting is part of large-scale synchronized activity, and this 'proper' burst mode transmits state-dependent information to the cortex, different from single spikes[6,8,23,40]. During activated states, however, single-spike and burst responses may relay the same visual information, only with different efficiencies[41]. The mixing of single-spike and burst responses to excitatory stimuli, as well as the more graded aspect of bursts, suggest that with background synaptic activity, there is indeed no clear distinction between single spikes and bursts. This may actually be advantageous for the relay of visual information: instead of a step-like input-output curve with limited coding capabilities for different input strengths, a linear response curve across the whole input range is generated by combining single and burst responses, suggesting that they convey the same type of information to the cortex during activated states.

Thalamic neurons share with cortical neurons the probabilistic aspect of responses under synaptic noise. This probabilistic nature of the thalamic relays is indeed realistic[15,42,43] if we consider that many thalamocortical cells converge on individual cortical cells[33,44,45], enabling those 'receiver' cells to collect many thalamocortical inputs (each of them firing one or several spikes in response to their sensory input) and to extract the probability function for a given stimulus.

Finally, these findings support the idea that corticothalamic synapses have a powerful role in controlling information transfer by the thalamus. It is known that corticothalamic feedback constitutes the primary source of synapses in the thalamus—one order of magnitude larger than synapses from peripheric axons[1,2]. Despite this anatomical fact, the feedforward view is still prominent: the thalamus is often considered as a 'relay' of information to cortex. By regulating the intensity of background activity, the cortex could exert a fast and efficient control of the thalamic relay—through instantaneous adjustment of gain and of bursting probability—which may be related to focused attention mechanisms (see also refs. 4, 28 and 46).

METHODS

We prepared LGNd slices (350 μm) from adult guinea-pigs as previously described[11]. We placed the slices at 34.5–35.5 °C in an interface style recording chamber (Fine Science Tools). The bathing medium contained (in mM): NaCl (126); KCl (2.5); $MgSO_4$ (1.2); NaH_2PO_4 (1.25); $CaCl_2$ (2); $NaHCO_3$ (26); and dextrose (10) and was aerated with 95% O_2 and 5% CO_2 to a final pH of 7.4. We made intracellular electrodes on a Sutter Instruments P-87 micropipette puller from medium-walled glass (World Precision Instruments, 1BF100). The electrodes were filled with 1.2 M potassium acetate and beveled (Sutter Instruments BV-10M) to resistances of 90–100 MÙ. We recorded at 10 kHz with an Axoclamp-2B amplifier (Axon instruments) in discontinuous current clamp (switching rate 2.5–3.5 kHz), using dynamic clamp[26].

Dynamic clamp and modeling techniques. Synaptic inputs were generated using a real-time version (Y. Le Franc, B. Foutry, F. Nagy & G. Le Masson, *Soc. Neurosci. Abstr.* 927.18, 2001) of the NEURON simulation environment[47] in combination with a programmable digital signal processor board M67 (Innovative Instruments), to achieve fast calculation and injection of dynamic-clamp currents (0.1 ms time step). We injected two types of simulated synaptic inputs, 'signal' and 'background', as conductances into thalamocortical cells using dynamic clamp[26]. The excitatory input from retinal ganglion cells (signal)[22] was modeled from the activation and inactivation kinetics of AMPA receptors[48] with randomized peak conductances (1–80 nS; step size: 2 nS). We fixed the stimulation frequency (5, 10 and 20 Hz) and randomized input amplitudes to analyze frequency-dependent effects separately. We also used Poisson-distributed inputs[31] of constant amplitude to approximate physiological input. To simulate the background synaptic input ('synaptic noise'), we used a fluctuating conductance model, mimicking the effect of thousands of stochastically glutamate- and GABA-releasing synapses[27]. These excitatory and inhibitory conductances were simulated as independent stochastic processes, assuming that the influence of the cortex on relay cells is a mixture of uncorrelated excitatory and inhibitory postsynaptic potentials (**Supplementary Methods** online). We validated the accuracy of the dynamic clamp conductance–based noise injection (i) by directly comparing the voltage fluctuations in real and model cells in response to injection of identical noise (**Supplementary Fig. 3** online), and (ii) by comparing natural and artificial (dynamic-clamp generated) synaptic noise in the same cells[49].

Data analysis and statistics. A spike was considered as a response to the input when it occurred within 20 ms after the stimulus onset. We analyzed input-output relations using spike probabilities instead of frequencies (see also **Supplementary Methods**). Spike probability was calculated as the number of EPSPs per given input level that generated at least one spike. We also considered the 'average total spike output' by taking into account all spikes of burst responses (interspike intervals <5 ms). To measure statistical significance, we performed single- and multifactorial analyses of variance (ANOVA; JMP software, SAS Institute). These tests were of the repeated-measures type in cases where all cells were submitted to the complete set of conditions, and of the independent type in the remaining cases. In the remaining cases, we assumed independence of conditions. We carried out post-hoc comparisons with non-parametric Wilcoxon rank-sum tests, using the software 'Instat' (University of Reading). Comparisons were of the unpaired, two-sided type, unless stated otherwise. We determined the significance of correlation according to a table of Pearson's *r*-values.

Note: Supplementary information is available on the Nature Neuroscience website.

ACKNOWLEDGMENTS

We thank M. Rudolph, G. Sadoc and L. Focsa for help with computation and Z. Piwkowska and D. Shulz for comments on the manuscript. This work was supported by the Centre National de la Recherche Scientifique, the Human Frontier Science Program, the European Commission (IST-2001-34712) and the Action Concertée Initiative 'Neurosciences integratives et computationnelles'. J.W. is the recipient of a European Union Marie Curie fellowship.

COMPETING INTERESTS STATEMENT

The authors declare that they have no competing financial interests.

Published online at http://www.nature.com/natureneuroscience/
Reprints and permissions information is available online at http://npg.nature.com/reprintsandpermissions/

1. Erisir, A., Van Horn, S.C. & Sherman, S.M. Relative numbers of cortical and brainstem inputs to the lateral geniculate nucleus. *Proc. Natl. Acad. Sci. USA* **94**, 1517–1520 (1997).
2. Van Horn, S.C., Erisir, A. & Sherman, S.M. Relative distribution of synapses in the A-laminae of the lateral geniculate nucleus of the cat. *J. Comp. Neurol.* **416**, 509–520 (2000).
3. Sherman, S.M. & Koch, C. The control of retinogeniculate transmission in the mammalian lateral geniculate nucleus. *Exp. Brain Res.* **63**, 1–20 (1986).
4. Koch, C. The action of the corticofugal pathway on sensory thalamic nuclei: a hypothesis. *Neuroscience* **23**, 399–406 (1987).
5. Ahissar, E., Haidarliu, S. & Zacksenhouse, M. Decoding temporally encoded sensory input by cortical oscillations and thalamic phase comparators. *Proc. Natl. Acad. Sci. USA* **94**, 11633–11638 (1997).
6. Sherman, S.M. Tonic and burst firing: dual modes of thalamocortical relay. *Trends Neurosci.* **24**, 122–126 (2001).
7. Sillito, A.M. & Jones, H.E. Corticothalamic interactions in the transfer of visual information. *Phil. Trans. R. Soc. Lond. B* **357**, 1739–1752 (2002).
8. McCormick, D.A. & Bal, T. Sleep and arousal: thalamocortical mechanisms. *Annu. Rev. Neurosci.* **20**, 185–215 (1997).
9. Jahnsen, H. & Llinas, R. Electrophysiological properties of guinea-pig thalamic neurones: an *in vitro* study. *J. Physiol. (Lond.)* **349**, 205–226 (1984).
10. Llinas, R.R. The intrinsic electrophysiological properties of mammalian neurons: insights into central nervous system function. *Science* **242**, 1654–1664 (1988).
11. Le Masson, G., Renaud-Le Masson, S., Debay, D. & Bal, T. Feedback inhibition controls spike transfer in hybrid thalamic circuits. *Nature* **417**, 854–858 (2002).
12. Steriade, M. Impact of network activities on neuronal properties in corticothalamic systems. *J. Neurophysiol.* **86**, 1–39 (2001).
13. Destexhe, A., Rudolph, M. & Pare, D. The high-conductance state of neocortical neurons *in vivo*. *Nat. Rev. Neurosci.* **4**, 739–751 (2003).
14. Ho, N. & Destexhe, A. Synaptic background activity enhances the responsiveness of neocortical pyramidal neurons. *J. Neurophysiol.* **84**, 1488–1496 (2000).
15. Anderson, J.S., Lampl, I., Gillespie, D.C. & Ferster, D. The contribution of noise to contrast invariance of orientation tuning in cat visual cortex. *Science* **290**, 1968–1972 (2000).
16. Chance, F.S., Abbott, L.F. & Reyes, A.D. Gain modulation from background synaptic input. *Neuron* **35**, 773–782 (2002).
17. Shu, Y., Hasenstaub, A., Badoual, M., Bal, T. & McCormick, D.A. Barrages of synaptic activity control the gain and sensitivity of cortical neurons. *J. Neurosci.* **23**, 10388–10401 (2003).
18. Larkum, M.E., Senn, W. & Luscher, H.R. Top-down dendritic input increases the gain of layer 5 pyramidal neurons. *Cereb. Cortex* **14**, 1059–1070 (2004).
19. Contreras, D., Timofeev, I. & Steriade, M. Mechanisms of long-lasting hyperpolarizations underlying slow sleep oscillations in cat corticothalamic networks. *J. Physiol.* **494**, 251–264 (1996).
20. Wilson, J.R., Friedlander, M.J. & Sherman, S.M. Fine structural morphology of identified X- and Y-cells in the cat's lateral geniculate nucleus. *Proc. R. Soc. Lond. B* **221**, 411–436 (1984).
21. Liu, X.B., Honda, C.N. & Jones, E.G. Distribution of four types of synapse on physiologically identified relay neurons in the ventral posterior thalamic nucleus of the cat. *J. Comp. Neurol.* **352**, 69–91 (1995).
22. Sherman, S.M. & Guillery, R.W. The role of the thalamus in the flow of information to the cortex. *Phil. Trans. R. Soc. Lond. B* **357**, 1695–1708 (2002).
23. Steriade, M., Jones, E.G. & McCormick, D.A. *Thalamus* Vol. 1 (Elsevier, Amsterdam, 1997).
24. Destexhe, A., Neubig, M., Ulrich, D. & Huguenard, J. Dendritic low-threshold calcium currents in thalamic relay cells. *J. Neurosci.* **18**, 3574–3588 (1998).
25. Destexhe, A. & Sejnowski, T.J. The initiation of bursts in thalamic neurons and the cortical control of thalamic sensitivity. *Phil. Trans. R. Soc. Lond. B* **357**, 1649–1657 (2002).
26. Prinz, A.A., Abbott, L.F. & Marder, E. The dynamic clamp comes of age. *Trends Neurosci.* **27**, 218–224 (2004).
27. Destexhe, A., Rudolph, M., Fellous, J.M. & Sejnowski, T.J. Fluctuating synaptic conductances recreate *in vivo*-like activity in neocortical neurons. *Neuroscience* **107**, 13–24 (2001).
28. Sillito, A.M., Jones, H.E., Gerstein, G.L. & West, D.C. Feature-linked synchronization of thalamic relay cell firing induced by feedback from the visual cortex. *Nature* **369**, 479–482 (1994).
29. McCormick, D.A. & Feeser, H.R. Functional implications of burst firing and single spike activity in lateral geniculate relay neurons. *Neuroscience* **39**, 103–113 (1990).
30. Perez-Reyes, E. Molecular physiology of low-voltage-activated t-type calcium channels. *Physiol. Rev.* **83**, 117–161 (2003).
31. Troy, J.B. & Robson, J.G. Steady discharges of X and Y retinal ganglion cells of cat under photopic illuminance. *Vis. Neurosci.* **9**, 535–553 (1992).
32. Turner, J.P., Leresche, N., Guyon, A., Soltesz, I. & Crunelli, V. Sensory input and burst firing output of rat and cat thalamocortical cells: the role of NMDA and non-NMDA receptors. *J. Physiol. (Lond.)* **480**, 281–295 (1994).
33. Usrey, W.M., Reppas, J.B. & Reid, R.C. Paired-spike interactions and synaptic efficacy of retinal inputs to the thalamus. *Nature* **395**, 384–387 (1998).
34. Lu, S.M., Guido, W. & Sherman, S.M. Effects of membrane voltage on receptive field properties of lateral geniculate neurons in the cat: contributions of the low-threshold Ca^{2+} conductance. *J. Neurophysiol.* **68**, 2185–2198 (1992).
35. Ramcharan, E.J., Gnadt, J.W. & Sherman, S.M. Burst and tonic firing in thalamic cells of unanesthetized, behaving monkeys. *Vis. Neurosci.* **17**, 55–62 (2000).
36. Weyand, T.G., Boudreaux, M. & Guido, W. Burst and tonic response modes in thalamic neurons during sleep and wakefulness. *J. Neurophysiol.* **85**, 1107–1118 (2001).
37. Leresche, N., Hering, J. & Lambert, R.C. Paradoxical potentiation of neuronal T-type Ca^{2+} current by ATP at resting membrane potential. *J. Neurosci.* **24**, 5592–5602 (2004).
38. Hirsch, J.C., Fourment, A. & Marc, M.E. Sleep-related variations of membrane potential in the lateral geniculate body relay neurons of the cat. *Brain Res.* **259**, 308–312 (1983).
39. Guido, W. & Weyand, T. Burst responses in thalamic relay cells of the awake behaving cat. *J. Neurophysiol.* **74**, 1782–1786 (1995).
40. Steriade, M. To burst, or rather, not to burst. *Nat. Neurosci.* **4**, 671 (2001).
41. Reinagel, P., Godwin, D., Sherman, S.M. & Koch, C. Encoding of visual information by LGN bursts. *J. Neurophysiol.* **81**, 2558–2569 (1999).
42. Lewis, J.E. Sensory processing and the network mechanisms for reading neuronal population codes. *J. Comp. Physiol. A* **185**, 373–378 (1999).
43. Barber, M.J., Clark, J.W. & Anderson, C.H. Neural representation of probabilistic information. *Neural Comput.* **15**, 1843–1864 (2003).
44. Tanaka, K. Organization of geniculate inputs to visual cortical cells in the cat. *Vision Res.* **25**, 357–364 (1985).
45. Alonso, J.M., Usrey, W.M. & Reid, R.C. Precisely correlated firing in cells of the lateral geniculate nucleus. *Nature* **383**, 815–819 (1996).
46. Montero, V.M. Amblyopia decreases activation of the corticogeniculate pathway and visual thalamic reticularis in attentive rats: a 'focal attention' hypothesis. *Neuroscience* **91**, 805–817 (1999).
47. Hines, M.L. & Carnevale, N.T. The NEURON simulation environment. *Neural Comput.* **9**, 1179–1209 (1997).
48. Destexhe, A., Mainen, Z.F. & Sejnowski, T.J. Kinetic models of synaptic transmission. in *Methods in Neuronal Modeling* 2nd edn. (eds. Koch, C. & Segev, I.) Ch. 1, 1–26 (MIT Press, Cambridge, Massachusetts, 1998).
49. Rudolph, M., Piwkowska, Z., Badoual, M., Bal, T. & Destexhe, A. A method to estimate synaptic conductances from membrane potential fluctuations. *J. Neurophysiol.* **91**, 2884–2896 (2004).